

Mechanisms of Particle Transport Acceleration in Porous Media

M. Panfilov⁽¹⁾, I. Panfilova⁽¹⁾ and Y. Stepanyants⁽²⁾

⁽¹⁾ *LEMMA, Nancy-Université, CNRS, France*
mikhail.panfilov@ensg.inpl-nancy.fr

⁽²⁾ *ANSTO, PMB 1, Menai (Sydney), 2234, NWS, Australia,*
Yury.Stepanyants@ansto.gov.au

24 November, 2006

Abstract. Experimental data show that the groundwater transport of radionuclides in porous media is frequently facilitated when accompanied with colloid particles. This is usually explained by the size exclusion mechanism which implies that the particles move through the largest pores where the flow velocity is higher.

We call attention to three other mechanisms which influence the colloid particle motion, while determining both the probable transport facilitation and retardation. First of all, it is shown that the transport facilitation may be significantly reduced and even transformed into a retardation due to the growth of the effective suspension viscosity (a friction-limited facilitation). Secondly, we will show that the transport of particles through the largest pores can be retarded due to a reduced connectivity of the large-pore cluster (a percolation-breakup retardation). Thirdly, we highlight the Fermi mechanism of acceleration known in statistical physics which is based on the elastic collisions between particles. All three effects are analyzed in terms of the velocity enhancement factor, by using statistical models of porous media in the form of a capillary bundle and a 3D capillary network. Optimal and critical regimes of velocity enhancement are quantified. Estimations show that for realistic parameters, the maximal facilitation of colloid transport is close to the experimentally observed data.

Keywords: groundwater; particle; transport; radionuclides; colloid; averaging; porous media; collisions; effective viscosity; Fermi acceleration; percolation; capillary network; enhancement factor

Introduction

The colloid suspension transport in porous media is a basic phenomenon observed in some industrial technologies and environmental technologies of water treatment from a radioactive and biological pollution, waterflooding of oil reservoirs, flow through filters, separation processes in chemical engineering, and others.

ABOUT THE FACILITATION EFFECT

Various authors observed that the transport of radionuclides by groundwater is sufficiently facilitated when accompanied with the colloid

© 2010 *Kluwer Academic Publishers. Printed in the Netherlands.*

particle transport. In fact, numerous observations, both in laboratory and in-situ, show that particles frequently have a greater velocity than the carrying liquid and move over greater distances than it is predicted by widely used models of single-phase solute transport. The ratio of the particle velocity to that of the carrying liquid is called the velocity enhancement factor.

Colloids are very fine particles (such as clay minerals, metallic oxides, viruses, bacteria, and organic macromolecules) whose size is between 1 and 1000 nm (McCarthy & Zachara, 1989) and that have a high specific surface depending on their size. Their chemical behavior is dominated by superficial processes (Moridis *et al*, 2003), and can have a high sorption capacity for the contaminants.

In several studies on colloid suspension transport as in (Moridis *et al*, 2003) an in-situ propagation of high-level nuclear waste at Yucca Mountain, Nevada, was studied. It was found that the radioactive colloids coming from the potential repository move faster than predicted, and reach the water table earlier and over a larger area in the southern part of the potential repository than in the remaining part. The authors give some reasons for this effect: infiltration and percolation distributions; the presence of highly conductive splays in the southern part of the potential repository; the presence of the zones of low permeability in the northern part of the potential repository. They also found that the greater the size of colloid particles the faster their movement. For example, the 450 nm colloidal particles move with 1.5 time average velocity of water.

In the study of plutonium (Pu) at Nevada (Kersting *et al*, 1999), the measured distance of Pu transport was revealed to be much greater than that predicted by classic models. Another study on plutonium and americium was released by (Penrose *et al*, 1990) in Mortandad Canyon, within the site of Los Alamos National Laboratory. They observed both plutonium and americium in the monitoring wells as far as 3390 m downstream from the discharge, while the laboratory studies predicted their movement to be limited to a few meters.

In the laboratory experiments where the contaminant colloid transport was studied it was confirmed that the mobile colloid particles can facilitate the transport of inorganic contaminants in natural porous media: (Grolimund *et al*, 1996), (Grolimund *et al*, 1998), (Ryan & Elimelech, 1996). In (Grolimund *et al*, 1998), the measured increase in particle velocity was of about 1.45 comparing to the velocity of the conservative tracer. They explain this effect by a size exclusion mechanism: the small pores being inaccessible for particles, the colloids are transported through a more permeable subdomain than water. The authors also observed that the dispersivity of colloid particles (both the

natural ones and the artificial ones made of latex) was higher than that of the conservative tracer.

One of the last publications related to the flow of colloid suspensions in columns was done by (Benamar *et al*, 2005). The paper deals with the matter transport and deposition of suspensions in saturated porous media. The authors used short-pulse tests to inject a conservative tracer and two types of suspended particles in a laboratory column: Rilsan and silt. Rilsan particles are artificial ones ranging between 2 and 50 μm with a mode of 25 μm , and silt particles are natural ones ranging between 2 and 40 μm with a mode of 15 μm . The Rilsan particles were used because of their density approaching that of water. From these tests it was noted that the particles in suspension are transported faster than the tracer. The ratio between the particles velocity and the dissolved tracer velocity was found to be close to 1.1.

Massei *et al.* (2002) also observed that large colloidal particles were transferred faster than fine particles. This fact confirms a very significant role of the size exclusion mechanism in colloidal transport.

According to (Kim, Zeh and Delakovitz, 1992) and (Buddemeier and Hunt, 1988), the measured velocity gain constitutes about 1.5.

The effect of acceleration of transported particles is clearly registered in petroleum literature dealing with the polymer flow. Polymers are injected with water into an oil reservoir in order to increase the oil displacement efficiency by increasing the effective water viscosity and thus by reducing the displacement instability, (Pope, 1980), (Sorbie, 1991).

A more detailed review of the experimental and theoretical results on transport facilitation may be found in (Sen & Khilar, 2006) and (Sorbie, 1991).

MECHANISMS OF TRANSPORT FACILITATION

Two explanations of colloid transport facilitation for electrically neutral particles can be found in the literature: the size exclusion mechanism and the effect of hydrodynamic chromatography.

The size exclusion mechanism is one of the principal causes of the transport facilitation. This mechanism consists in the fact that the colloid particles are transported through more permeable pathways than water as the fine pores are not accessible for large particles. Obviously, the pore-scale flow velocity in large pores is higher than that in the remaining part of the porous medium. This mechanism cannot be reduced by increasing the total flow velocity, as the inaccessibility of fine pores is invariable with respect to any velocity.

The effect of hydrodynamic chromatography can be illustrated by the transport in a capillary tube (Corapcioglu & Jiang, 1993). For a Poiseuille flow through a straight circular tube of constant diameter, the velocity profile across a cross-section is parabolic with a maximum at the tube center and the average velocity equals to one half maximum velocity. Due to its finite size a solid particle is excluded from the slowest region just near the tube wall and migrates at a higher velocity than the average velocity in the capillary tube.

The chromatographic effect is frequently mentioned in the literature as the basic mechanism responsible for the transport facilitation, however, the estimations made in (Dodds, 1982) show that this effect may produce an increase in the transport velocity by the factor of 1.08 at the most.

The explanation in terms of the size exclusion mechanism was also used in (Kim, Zeh and Delakovitz, 1992), (Buddemeier and Hunt, 1988), (Von Gunten, Waber and Krabenbuhl, 1988), (Lieser *et al*, 1990) and other papers.

The size exclusion is the basic mechanism that explains the acceleration of long polymer molecules injected with water into oil reservoirs, which was observed and analyzed in (Gilham & MacMillan, 1987), (Small, 1974), (Sorbie, 1991), (Sorbie, Parker & Clifford, 1987), and (Teeuw & Hesseling, 1980).

Although this explanation is very popular in geosciences, it is insufficient for the interpretation of existing experimental data. Several attempts were undertaken to improve physical models. In particular, it was suggested to introduce kinetic effects in the above model of colloids straining (van de Weerd and Leijnse, 1997).

In the present paper we re-examine the colloid straining model, taking into account an increase of the effective fluid viscosity in presence of colloids and the connectivity reduction of the pore cluster occupied with the particles. These effects reduce the average velocity of colloids so that the velocity gain with respect to the mean fluid velocity can be completely removed. These effects are analyzed mathematically with the help of statistic models of porous media.

It is also assumed that the radionuclides are adsorbed on the colloid particles. However, the adsorptivity depends on the chemical composition of colloids and radionuclides and can vary within a wide range. In the case of a low adsorptivity the collisions between a radionuclide and a colloid particle can be almost elastic, which leads to a momentum and energy exchange between such particles. As a result, the average velocity of small radionuclide particles can grow due to the effect of the Fermi acceleration (Zaslavsky, 1985; Sagdeev *et al*, 1988). The neces-

sary conditions of such acceleration are calculated, and the quantitative estimation of the velocity enhancement is obtained.

1. Enhancement factor

1.1. GENERAL DEFINITION OF THE ENHANCEMENT FACTOR

The transport facilitation of colloid particles can be described in terms of the velocity enhancement factor which is defined according to the differential equations describing the single phase transport of two species (water and colloids) at two different transport velocities on the macroscale:

$$\frac{\partial C_w}{\partial t} + U_w \frac{\partial C_w}{\partial x} = f_w, \quad \frac{\partial C_p}{\partial t} + U_p \frac{\partial C_p}{\partial x} = f_p \quad (1)$$

where C_w and C_p are the concentrations of water and particles respectively, U_w and U_p are the macroscopic transport velocities of water and particles (the volume averages). The equation system is written in the particular case of mono-dimensional flow along the axis x . Various physical effects related to the diffusion, filtration and probably sorption and segregation are hidden in the source terms f_w and f_p . The effect of porosity reduction due to particle retention is neglected.

Note that the system will have many different velocities if the diffusion is taken into account as the advection velocity is no longer equal to the true transport velocity of each species. In order to avoid such a situation with multiple velocities which create difficulty in understanding the main studied effect, we will neglect the diffusion in this paper.

As water is present in all the pores, then $U_w = U$ where U is the macroscopic flow velocity for the overall fluid in all the pores. This velocity is assumed to be known a priori, which is not the case of the second velocity, U_p . Indeed, this velocity is usually different from U , as the particles are present only in a part of pores, but U_p cannot be independent of U : the faster the total flow, the faster the particle transport. So, U_p is usually defined as proportional to U with a proportionality coefficient ω called the velocity enhancement factor:

$$\omega \equiv \frac{U_p}{U} \quad (2)$$

Parameter ω is assumed to depend only on the medium structure and particle radius, but to be independent of the total flow velocity and colloid concentration. To calculate this factor, some empirical correlations are usually used, (James & Chrysikopoulos, 2003).

We develop a theoretical microscale approach which provides some qualitative and quantitative theoretical results for the enhancement factor that can depend on the colloid concentration and shows a non-trivial behaviour.

1.2. ENHANCEMENT FACTOR AND MEDIUM MICROSTRUCTURE

Let the total pore ensemble be Ω , the ensemble of pores occupied with particles be Ω_p , the total ensemble of particles be \mathcal{P} , while the ensemble of particles in i^{th} pore be \mathcal{P}_i . The volume of a pore and a particle is denoted as v and v_p respectively. Let u be the local flow velocity in the given pore, u_p be the local transport velocity of a given particle. Let c be the local concentration of particles in a pore defined as the volume of all the particles present in this pore divided by the volume of this pore: $c_i = \sum_{j \in \mathcal{P}_i} v_{pj} / v_i$.

So the average total flow velocity and the average particle transport velocity defined as the volume averages over the pore volume are:

$$U = \frac{\sum_{i \in \Omega} u_i v_i}{\sum_{i \in \Omega} v_i}, \quad U_p = \frac{\sum_{j \in \mathcal{P}} u_{pj} v_{pj}}{\sum_{j \in \mathcal{P}} v_{pj}}$$

In the present paper we will assume, for the sake of simplicity, that: i) all the particles are identical, spherical and have the radius R , ii) the transport velocity of a particle is equal to the mean flow velocity of the surrounding water in this pore, so in a given pore all the particles have the same velocity; iii) the local concentration c of particles is identical in each pore where they are present ; iv) the particles can reduce the water flow velocity due to an increase in the effective fluid viscosity - such a retardation concerns both the water and the particles.

Within the scope of such assumptions, we obtain:

$$\sum_{j \in \mathcal{P}} u_{pj} v_{pj} = \sum_{i \in \Omega_p} u_i \sum_{j \in \mathcal{P}_i} v_{pj} = \sum_{i \in \Omega_p} u_i v_i c$$

Due to this, we obtain for the enhancement factor:

$$\omega = \frac{\sum_{i \in \Omega_p} u_i v_i \sum_{j \in \Omega} v_j}{\sum_{j \in \Omega} u_j v_j \sum_{i \in \Omega_p} v_i} \quad (3)$$

2. Friction-induced transport retardation

In the present section we consider the size exclusion mechanism while taking into account the effective viscosity increase for rather concentrated colloid suspensions. The straining of colloid particles in narrow pores determines a higher average velocity of particles with respect to the mean total fluid velocity as the particles are transported only through the largest pores. At the same time this effect is always accompanied with the effective viscosity increase due to the presence of solid particles. This reduces the velocity enhancement factor and even can retard the particle transport. Due to this an optimal set of parameters exists when the average colloids velocity has a maximum. To capture all these effects which are independent of the pore network connectivity the model of a bundle of random non-connected capillaries is sufficient.

2.1. TRANSPORT MODEL THROUGH A RANDOM CAPILLARY BUNDLE

Let us assume that the porous medium consists of a bundle of capillary tubes of random radii, with the density of radius distribution $f(r)$ normalized to one: $\int_0^{\infty} f(r) dr = 1$.

Suppose also that the viscous fluid moves through the bundle under a constant pressure gradient $|dp/dx| = J$ at a relatively small velocity, so that the Reynolds number $Re < 1$. Then, the well-known Hagen–Poiseuille flow with the parabolic profile in each tube is realized ((Happel and Brenner, 1965), (Landau & Lifshitz, 1988)) which is described by the following relation for the mean flow velocity u in a pore-tube:

$$u(r) = \frac{Jr^2}{8\mu} \quad (4)$$

where r is the tube radius, μ is the dynamic fluid viscosity.

Due to the presence of colloid particles in some pores, the effective fluid viscosity in those pores is different from the viscosity of pure fluid and depends on the local particle concentration c : $\mu = \mu(c)$. The volumetric particle concentration c is defined as the ratio of the total volume of colloid particles in the capillary tube to the total volume of the tube. Function $\mu(c)$ is presented in the next subsection.

If the colloid particles are uniform and have radius R , then such particles can be transported only through those pores whose radii are larger than R . All the tubes can be divided into two classes: i) class Ω_p consists of the large tubes: $R < r < \infty$, where the viscosity is modified due to the presence of colloid particles; and ii) class $\Omega - \Omega_p$ of narrow

tubes: $0 \leq r \leq R$, where no particles are present and the flow viscosity is equal to the viscosity of the pure fluid, $\mu_0 = \mu(0)$.

From (3) it follows for the enhancement factor:

$$\omega(R, c) \equiv \frac{\frac{1}{\mu(c)} \int_R^\infty r^4 f(r) dr \int_0^\infty r^2 f(r) dr}{\left[\frac{1}{\mu(0)} \int_0^R r^4 f(r) dr + \frac{1}{\mu(c)} \int_R^\infty r^4 f(r) dr \right] \int_R^\infty r^2 f(r) dr}. \quad (5)$$

To complete this formula, one should determine the effective fluid viscosity $\mu(c)$ of a fluid containing colloid particles.

In practice one can measure rather the total concentration of particles in fluid, C , defined as the ratio of the particle volume to the total pore volume. The relation between c and C is as follows:

$$c = \frac{C \int_0^\infty f(r) r^2 dr}{\int_R^\infty f(r) r^2 dr} \quad (6)$$

2.2. EFFECTIVE VISCOSITY OF A COLLOID SUSPENSION

It is well known that the effective fluid viscosity increases when the fluid contains solid particles (Landau & Lifshitz, 1988). For the simplest case when the particles have equal sizes and the shape of prolate and oblate ellipsoids with the half-axes ξ and $\eta = \zeta$, the effective fluid viscosity is calculated on the bases of the Einstein formula:

$$\mu = \mu_0 (1 + Ac), \quad c \equiv \frac{4}{3} \pi \xi \eta^2 n \quad (7)$$

where μ_0 is, as earlier, the dynamic viscosity of pure fluid; n is the number of particles in a unit volume; for spherical particles, c is the local volumetric particle concentration in the pores occupied by colloids; parameter A depends on the ratio ξ/η as shown in Fig. 1 (the dots represent data from (Landau & Lifshitz, 1988), while the solid curve is the best fit approximation). The minimum value $A = 2.5$ corresponds to spherical particles for which $\xi = \eta = \zeta$. Parameter A remains almost constant when ξ/η varies in the range $0.5 < a/b < 2$.

System (5), (7) and (6) is closed if the total particle concentration is known.

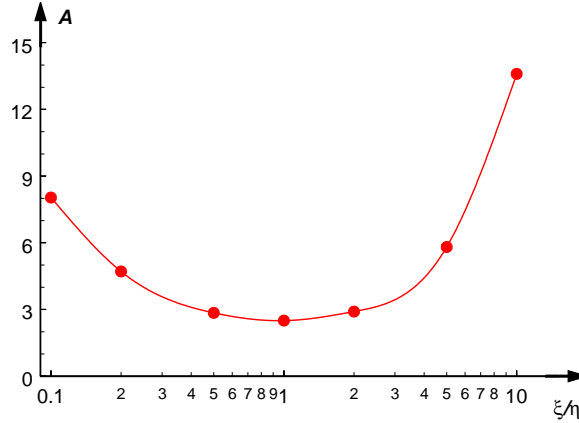


Figure 1. Parameter A vs. the ratio between the particles semi-axes

2.3. ENHANCEMENT FACTOR AND IDEAL ENHANCEMENT FACTOR

By substituting the expression for the effective viscosity, Eq. (7), into Eq. (5), one obtains the formula for the enhancement factor:

$$\omega(R, C) = \frac{\lambda}{\nu + AC(1 - \lambda)} \quad (8)$$

where C is the total particle concentration, ν is the volume fraction of large pores, while λ is the volume fraction of the volumes of the large pores:

$$\lambda(R) \equiv \frac{\int_0^{\infty} r^4 f(r) dr}{\int_0^{\infty} r^4 f(r) dr}, \quad \nu(R) \equiv \frac{\int_0^{\infty} r^2 f(r) dr}{\int_0^{\infty} r^2 f(r) dr}, \quad \rho \equiv R/\langle r \rangle \quad (9)$$

Note that relation (6) between the local and the global concentrations (c and C respectively) becomes:

$$C = \nu c$$

Let us calculate function $\omega(R, C)$ for three kinds of pipe radii distribution frequently used for practical purposes in the statistical description of porous media: i) the uniform distribution which is simple to treat, but can only be examined as a coarse approximation to real media, ii) the Rayleigh distribution, which has an asymmetric form typical for real media, is one-parametric and allows to obtain analytical expressions, and iii) the log-normal distribution which is most widely

used in practice, is formally similar to the Rayleigh function but is two-parametric.

Let $\rho = R/\langle r \rangle$ be the ratio between the particle size and the mean pore size, $\langle r \rangle$ be the mean pore radius, and σ be the variance of radii.

1° Uniform distribution of pore radii:

$$f(r) = \begin{cases} 1/r_m, & 0 \leq r \leq r_m, \\ 0, & r > r_m, \end{cases}$$

where r_m is the maximum tube radius, while $\langle r \rangle = r_m/2$ is the mean pore radius.

Parameters λ and ν can be readily calculated:

$$\lambda = 1 - (\rho/2)^5, \quad \nu = 1 - (\rho/2)^3,$$

where $\rho = R/\langle r \rangle$.

2° Rayleigh distribution:

$$f(r) = 2\alpha r e^{-\alpha r^2}, \quad \alpha = \frac{\pi}{4\langle r \rangle^2}$$

Parameters λ and ν are:

$$\lambda = e^{-\pi\rho^2/4} \left(\pi^2\rho^4/32 + \pi\rho^2/4 + 1 \right), \quad \nu = e^{-\pi\rho^2/4} \left(\pi\rho^2/4 + 1 \right)$$

3° Log-normal distribution:

$$f(r) = \frac{1}{r\sqrt{2\pi s}} \exp\left(-\frac{\ln^2\left(\frac{r}{r_m}\right)}{2s}\right)$$

$$r_m = \langle r \rangle / \sqrt{\chi}, \quad s = \ln \chi, \quad \chi \equiv 1 + \left(\frac{\sigma}{\langle r \rangle}\right)^2$$

Parameters λ and ν are:

$$\lambda = \frac{1}{2} \left(1 - \operatorname{erf}\left(\frac{\ln \rho - 3.5s}{\sqrt{2s}}\right) \right), \quad \nu = \frac{1}{2} \left(1 - \operatorname{erf}\left(\frac{\ln \rho - 1.5s}{\sqrt{2s}}\right) \right)$$

Three distributions are shown in Fig. 2 for the same mean values and variances $\sigma^2 = \langle r \rangle^2(4 - \pi)/\pi$.

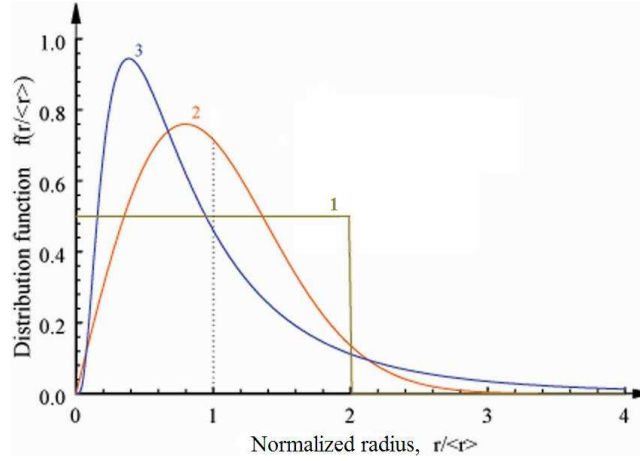


Figure 2. Various radius distributions: uniform (1), Rayleigh (2) and log-normal (3)

For these three kinds of distribution functions, the enhancement factor ω can be presented in terms of dimensionless colloid radius ρ and total particle concentrations C :

- uniform distribution:

$$\omega(\rho, C) = \frac{1 - (\rho/2)^5}{1 - (\rho/2)^3 + AC(\rho/2)^5} \quad (10)$$

- Rayleigh distribution:

$$\omega(\rho, C) = \frac{\pi^2 \rho^4 / 32 + \pi \rho^2 / 4 + 1}{\pi \rho^2 / 4 + 1 + AC(e^{\pi \rho^2 / 4} - \pi^2 \rho^4 / 32 - \pi \rho^2 / 4 - 1)} \quad (11)$$

- log-normal distribution:

$$\omega(\rho, C) = \frac{1 - \operatorname{erf}\left(\frac{\ln \rho - 3.5s}{\sqrt{2s}}\right)}{1 - \operatorname{erf}\left(\frac{\ln \rho - 1.5s}{\sqrt{2s}}\right) + AC\left(1 + \operatorname{erf}\left(\frac{\ln \rho - 3.5s}{\sqrt{2s}}\right)\right)} \quad (12)$$

Along with this, we introduce *the ideal enhancement factor* ω_0 , which corresponds to the ideal situation when the suspension viscosity is equal to that of pure water whatever the particle concentration. This

is equivalent to the limit of the examined relationships when $C = 0$:

$$\omega_0(\rho) = \frac{\lambda}{\nu} = \begin{cases} \frac{1 - (\rho/2)^5}{1 - (\rho/2)^3}, & \text{uniform distribution} \\ \frac{\pi^2 \rho^4 / 32 + \pi \rho^2 / 4 + 1}{\pi \rho^2 / 4 + 1}, & \text{Rayleigh} \\ \frac{1 - \operatorname{erf}\left(\frac{\ln \rho - 3.5s}{\sqrt{2s}}\right)}{1 - \operatorname{erf}\left(\frac{\ln \rho - 1.5s}{\sqrt{2s}}\right)}, & \text{log-normal} \end{cases} \quad (13)$$

Obviously, the ideal enhancement factor represents an upper estimation for the velocity enhancement.

The dependence of the enhancement factor on the normalized particle radius at various concentrations C is shown in Figs. 3a for the uniform distribution, 3b for the Rayleigh distribution, and 3c for the log-normal distribution. Note that $\rho = 1$ when the colloid particle radius is equal to the mean pore radius.

All the distribution shapes produce qualitatively similar results for the velocity enhancement factor. The quantitative differences depend only on the length of the distribution "tail": the longer the tail, the higher the role of the large pores that just determine the particle acceleration.

As seen, if the viscosity growth is neglected (curves 0), then the greater the particles, the higher the velocity enhancement effect. If the viscosity growth is taken in consideration, the results are different: an optimal particle size appears that determines acceleration. In particular, for concentrated suspensions, the maximal velocity enhancement is observed for particles whose size constitutes 1.5 - 2.5 of the mean pore radius.

The reduction of ω and even the particle retardation observed for large ρ are explained in the next section.

2.4. TRANSPORT RETARDATION

In all the cases when $\omega < 1$ the transport facilitation effect turns into a transport retardation. As seen from Fig. 3, the retardation is observed when the particle radius ρ exceeds a critical value, $\rho_c(c)$, which depends on the colloid concentration. The retardation is explained by the fact that the increase of the particle size leads to a reduction of the pore volume occupied by the particles. Due to this the local concentration grows if the total concentration is invariable. This determines an increase in

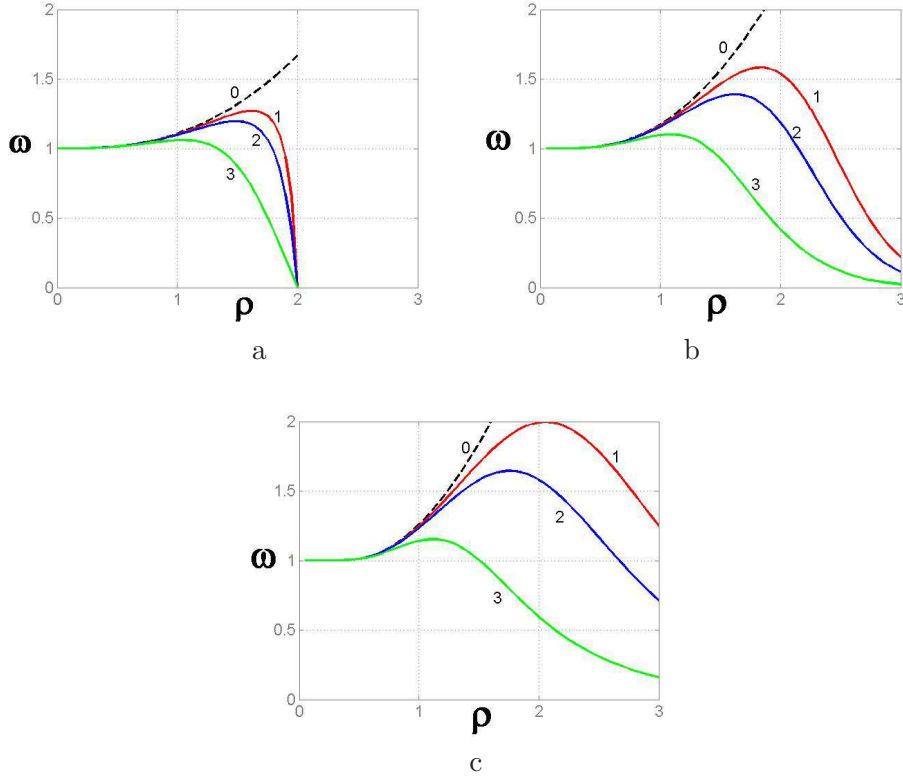


Figure 3. Velocity enhancement factor, $\omega(\rho, C)$, versus normalized particles radius ρ at various colloid concentrations C for the uniform (a), Rayleigh (b) and log-normal (c) distribution of tube radii. Dashed lines (0) correspond to the ideal enhancement factor. Solid lines: (1) $C = 0.05$; (2) $C = 0.1$; (3) $C = 0.5$.

the effective viscosity. Starting from the critical radius, the increase in viscosity becomes more significant than the velocity enhancement due to the size exclusion.

The critical radius of colloid particles may be obtained from Eq. (8) as a positive root of the transcendental equation:

$$\lambda(\rho_{cr}) - \nu(\rho_{cr}) - AC(1 - \lambda(\rho_{cr})) = 0 \quad (14)$$

which determines function $\rho_{cr}(C)$.

Along with the critical radius of colloid particles, an optimal particle radius may be determined as the value at which the velocity enhancement reaches its maximum. This radius can be found as the solution to the equation:

$$\frac{\partial \omega}{\partial \rho} = 0 \rightarrow \lambda'AC + \nu\lambda' - \nu'\lambda = 0, \quad (\cdot)' \equiv \frac{d}{d\rho} \quad (15)$$

The critical and the optimal dimensionless particle radii as the solutions to (14) and (15) are presented in Fig. 4 for the uniform (line 1) and the Rayleigh (line 2) distribution of pore radii.

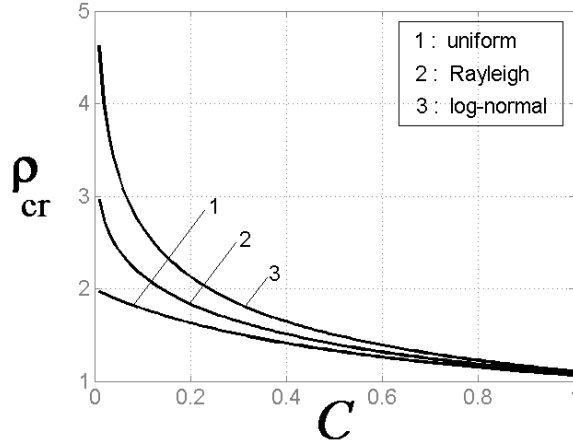


Figure 4. Critical dimensionless radius of colloid particles vs. total concentration C for the uniform (1), Rayleigh (2) and log-normal (3) distribution of pore radii

The optimal radius illustrates the similar qualitative behaviour but is lower than the critical one approximately by factor 0.8.

As seen, the optimal and the critical particle radii lie between 0.7 for concentrated colloid suspensions and 2–2.5 for diluted suspensions.

For all the distribution functions, the maximum enhancement factor reached at the optimal particle radius varies approximately from 1 to 2 depending on the colloid concentration. So, the experimentally observed values, ~ 1.5 , agree with our theoretical results.

3. Percolation-breakup retardation

The size exclusion mechanism implies that not all the pores are accessible to the colloid particles. The larger the particles, the higher their transport velocity in each pore, but the smaller the cluster of accessible pores becomes. The diminishing of the accessible cluster can lead to its entire breakup, which would determine the impossibility to transport the particles. So, the cluster connectivity plays a very significant role in the particle transport.

As the bundle model of porous media is incapable of taking into account the probable disconnections in pore clusters, we used the three-dimensional pore network model to analyze the influence of the cluster connectivity on the velocity enhancement/retardation.

3.1. MODEL DESCRIPTION

The numerical algorithm developed by the authors to describe multi-phase flows in a capillary network model of porous media is described in various preceding publications, for instance in (Panfilova, 2003) and (Panfilova and Panfilov, 2000).

Briefly, the geometrical model of porous medium represents a uniform cubic network of nodes connected by cylindrical capillary tubes, as shown in Fig. 5.

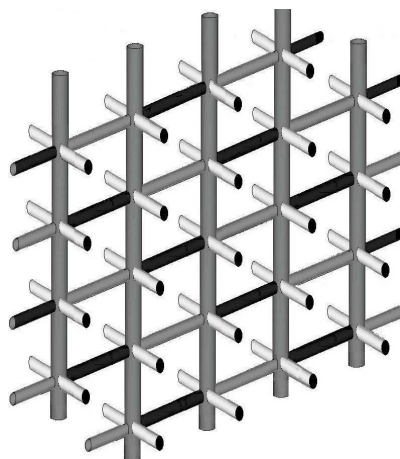


Figure 5. One range of the capillary network used as a micromodel of porous media.

The tube radius is considered as a stochastic stationary space function with a given global distribution, covariance function and mean value.

The generation of a stochastic random network was performed by using both the turning band method and the kriging described for instance in (Oh, 1998) and (Mantoglou & Wilson, 1982). The first one is based on constructing one realization of a stochastic field by using the given mean value and the covariance function. The second method uses the mean value and several pointed values of a realization as the initial information. Both methods provide a random 2D or 3D space function of pore radii. The example of a random radius field used in the simulations is shown in Fig. 7.

In all the examined cases the correlation length was lower than the size of the medium, due to this the medium could be examined as an ERV: elementary representative volume.

In a cubic or square porous medium whose structure is described above, a modification of the single phase flow is examined, when the fluid viscosity may be different in various pores. The flow in each pore

tube is described by the Poiseuille law, (4) in which J is the pressure difference ΔP_i along the examined pore i divided by its length l_p . The flow conservation applied to each node of pore intersection yields a system of recurrent equations formulated with respect to the node pressures:

$$\sum_i r_i^2 u_i = 0, \quad \rightarrow \quad \sum_i a_i \Delta P_i = 0; \quad a_i = \frac{r_i^4}{8\mu l_p}$$

with summing over all the pores crossed in the examined node; $a(r)$ is the parameter of hydraulic resistance such that $a_i = a(r_i)$.

The last equation can be rewritten in the following form for node (i, j) :

$$a_{i-\frac{1}{2},j} (P_{i-1,j} - P_{i,j}) + a_{i,j-\frac{1}{2}} (P_{i,j-1} - P_{i,j}) + \\ a_{i+\frac{1}{2},j} (P_{i+1,j} - P_{i,j}) + a_{i,j+\frac{1}{2}} (P_{i,j+1} - P_{i,j}) = 0$$

where $a_{i-\frac{1}{2},j}$ is the value of coefficient a affected to the pore whose center is $\{(i-1/2)\Delta h, j\Delta h\}$, with $\Delta h = l_p$; similar for $a_{i+\frac{1}{2},j}$ and so on.

This system may be considered as a discrete form of the differential Laplace equation at a variable coefficient $a(\vec{x})$:

$$\text{div}(a(\vec{x})\text{grad}P) = 0$$

The solution to this system is constructed by using the standard numerical methods of solving the elliptic equations.

We examined a cubic or a quadratic medium, which represents an ERV, with the following boundary conditions: a constant pressure at the inlet side, another constant pressure at the opposite outlet side and the no-flow conditions at all other sides. According to the homogenization theory, (Bakhvalov and Panasenko, 1989), such a problem represents a cell-problem which is needed to determine the effective flow parameters.

As a result of such a simulation we obtain the pressure field determined in each node.

3.2. P -CLUSTER AND THE PERCOLATION-BREAKUP EFFECT

As earlier we assume that all the particles are of the same radius R . So the overall pore space may be split into two clusters: i) a W -cluster that corresponds to narrow pores ($r < R$) in which only pure water flows; ii) a P -cluster consisting of large pores ($r > R$) in which colloid particles are present, Fig. 6.

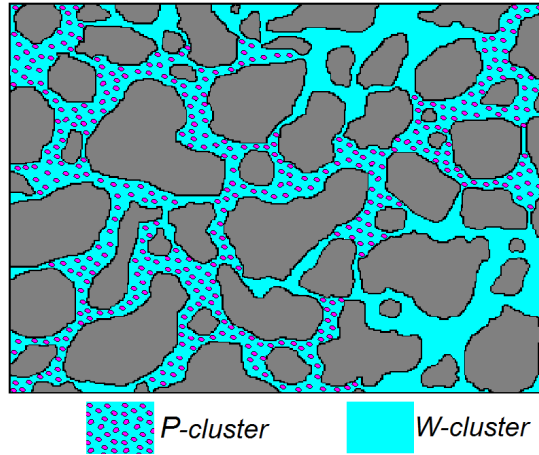


Figure 6. Two clusters of pores: P-cluster is occupied by particles, while W-cluster contains only pure water.

It has been observed that a significant part of large pores can not be occupied by particles, as they are blocked by narrow pores. This effect is typical for the percolation theory. Due to this, the particle velocity enhancement factor will be reduced.

For a given value of R and for a given field or pore radii, the selection of the P -cluster may be performed numerically, by using the procedure suggested first in (Entov *et al*, 1975) and developed in (Panfilova, 2003). This consists in the following:

- i Assigning to each pore of the classification index " $c1$ " (c means "colloid") if $r > R$.
- ii Detection of all the connected $c1$ -pores and assigning to them the index " $c2$ ". A pore is called connected if it has at least one neighboring $c1$ -pore.
- iii Detection of the $c2$ -pores in the inlet section of the medium and assigning to them the index " $c2_{inl}$ ".
- iv Detection of all the $c2$ -pores connected to $c2_{inl}$ and assigning to them the index $c3$.
- v Detection of all the $c3$ -pores in the outlet section of the medium and assigning to them the index $c3_{out}$.
- vi Detection of all the $c3$ -pores connected to $c3_{out}$ and assigning to them the index c .

The obtained c -pores represent a continuous P -cluster connected to the medium inlet and the outlet.

The larger the particles, the finer the P -cluster. Fig. 7 illustrates the successive reduction of the P -cluster (yellow) when the particle radius

decreases when calculated numerically for one of the media presented above.

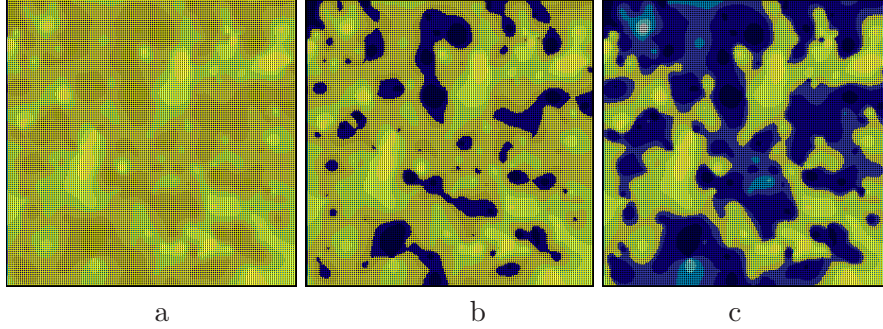


Figure 7. P -cluster reduction when the particle radius increases (The P -cluster is marked by clary colors, W -cluster is black): a,b,c correspond to $\rho = 0.01, 0.2, 0.7$ respectively

Such a simulation is independent of flow problem and requires to develop an individual simulator.

3.3. VECTOR ENHANCEMENT FACTOR

To calculate the enhancement factor in a 3D case, the definition of the enhancement factor (2) should be generalized, as the averaged velocity is now a vector. We will thus introduce a vector enhancement factor

$$\omega = \{\omega_1, \omega_2, \omega_3\}, \quad \omega_i = \frac{U_{pi}}{U_i} \quad (16)$$

(without summation over the repeating indexes) where U_i is the i^{th} component of the vector flow velocity \mathbf{U} averaged over the ensemble of all the pores, while U_{pi} is the i^{th} component of the particle vector velocity \mathbf{U}_p averaged over the ensemble of pores occupied with particles. As the simulated medium represents an ERV, then the ensemble average is taken over the overall medium.

According to the boundary-value conditions described in section 3 in the examined case, the macroscale flow is monodirectional (along x_1), so in this case it is sufficient to determine the only component $\omega \equiv \omega_1$ of the enhancement factor. To calculate the two velocities U_1 and U_{p1} it is sufficient to average the corresponding velocities over the sub-ensemble of pores oriented along the axis x_1 only.

Let all the pores be denoted as Ω , the P -cluster as Ω_p , the ensemble of all the pores oriented along x_1 be Ω_1 , the ensemble of P -cluster pores oriented along x_1 be Ω_{p1} . Then the enhancement factor is defined as

similar to (3):

$$\omega_1 = \frac{\sum_{i \in \Omega_{p1}} u_i v_i \sum_{j \in \Omega_1} v_j}{\sum_{j \in \Omega_1} u_j v_j \sum_{i \in \Omega_{p1}} v_i} \quad (17)$$

The average velocities are simulated in the following ways. Knowing the pressure difference field in the pore network and all the pores belonging to the P -cluster, we can calculate the sums in (17) by using the Poiseuille law for each pore (4):

$$\omega_1 = \frac{1}{\mu(C)} \frac{\sum_{i \in \Omega_{p1}} r_i^4 \Delta P_i \sum_{j \in \Omega_1} r_j^2}{\sum_{j \in \Omega_1} \frac{r_j^4}{\mu_j} \Delta P_j \sum_{i \in \Omega_{p1}} r_i^2} \quad (18)$$

where μ_j is equal either to $\mu(0)$ in W -pores, or to $\mu(C)$ in P -pores.

3.4. ENHANCEMENT FACTOR AND PERCOLATION-BREAKUP

The results of simulations based on the equation (18) are shown in Fig. 8.

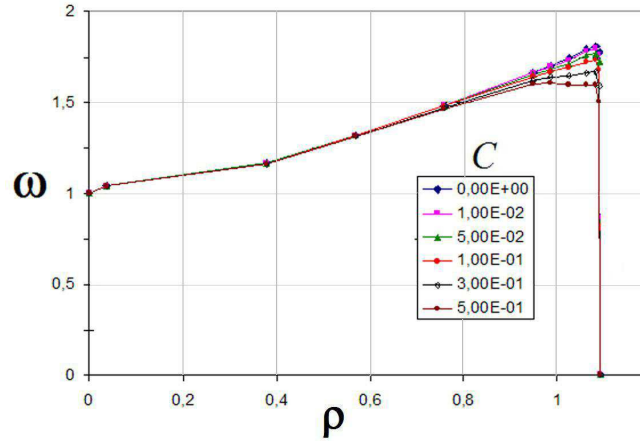


Figure 8. Enhanced factor ω vs. dimensionless particle radius ρ for various concentrations C .

In this case the critical particle radius determines the complete breakup of the P -cluster and the consecutive sharp reduction of the enhancement factor up to zero. As seen previously, such a breakup may be observed starting from a particle radius slightly greater than the mean pores size.

The percolation-break effect provokes a more important retardation than the effective viscosity growth.

4. Elastic particle collisions and stochastic Fermi acceleration

The radionuclides may also be accelerated due to their collisions with colloid particles without adsorption. Such a mechanism is quite different from the size exclusion mechanism analyzed above.

This mechanism is known as the Fermi acceleration and was originally suggested as an explanation of the acceleration of cosmic rays by magnetic clouds in the interstellar space (see the details in (Zaslavsky, 1985; Sagdeev *et al*, 1988)). According to this mechanism, if radionuclide molecules pass through a cloud of colloid particles, their velocity gradually increases on average. The effect happens due to the energy and momentum transfer from the colloid particles to radionuclides. Even in the case when the average velocity of colloids is smaller than that of radionuclides, their kinetic energy may be significantly larger due to a high difference between the particle masses. Moreover, the effect occurs even when the colloid particle do not move in average, but only oscillate around their equilibrium positions. This may happen, for example, when a large-size colloid particle blocks the entrance into a narrow throat and vibrates under the influence of water flowing around it.

The theory of this effect may be applicable to that class of particles for which the radionuclide adsorption by colloids is not significant and their collisions are almost elastic.

4.1. MECHANICS OF PARTICLE COLLISIONS

Let us consider the elementary act of a rigid centered collision between two particles of masses m_1 and $m_2 \gg m_1$. Let us assume that the particles trajectories lie along the same axis x which crosses the centers of both the particles. Let us assume for definiteness that the particles move towards one another before the collision, and bounce off each other after the collision (Fig. 9). Let V_{i0} and V_i be the particle velocities before and after the collision respectively.

The directions of the particles after the collision specified in the figure represent one of the probable configurations.

The momentum and energy balance equations are formulated in the following way:

$$m_1 V_{10} - m_2 V_{20} = -m_1 V_1 - m_2 V_2,$$

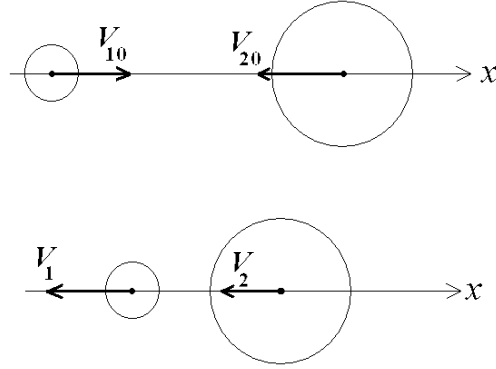


Figure 9. The outline of particle collision: a) before the collision; b) after the collision

$$m_1 V_{10}^2 + m_2 V_{20}^2 = m_1 V_1^2 + m_2 V_2^2,$$

where the first relation is the projection of the vector momentum balance equation to the axis x .

By introducing the ratios: $\varepsilon = m_1/m_2$ and $\delta = V_{20}/V_{10}$, one obtains a system of two equations with respect to two variables, V_1 and V_2 :

$$(\varepsilon - \delta) V_{10} = -V_2 - \varepsilon V_1, \quad (\varepsilon + \delta^2) V_{10}^2 = V_2^2 + \varepsilon V_1^2$$

The unique physically admissible solution to this system is

$$V_1 = \frac{1 + 2\delta - \varepsilon}{1 + \varepsilon} V_{10}, \quad V_2 = \frac{1 - \varepsilon - 2\varepsilon/\delta}{1 + \varepsilon} V_{20} \quad (19)$$

Let us assume now that the initial velocity of the small particle is positive, i.e., it moves to the right as shown in Fig. 9. Then only two kinds of collision are possible: i) a head-on collision ($\delta > 0$) and ii) a pursuing collision ($-1 < \delta < 0$) when the small particle overtakes the large one which also moves to the right rather than to the left. The case $\delta < -1$ stands for the absence of any collisions (a slowly moving small particle cannot overtake the large particle moving at a higher velocity in the same direction) and may be excluded from consideration.

As follows from Eq. (19), the velocity of the small particle increases after the collision $|V_1| > V_{10}$, if the following condition is verified:

$$\left| \frac{1 + 2\delta - \varepsilon}{1 + \varepsilon} \right| > 1 \quad (20)$$

For a head-on collision, this condition leads to:

$$\varepsilon < \delta, \quad (21)$$

which means that the large particle has a greater momentum: $m_2 V_{20} > m_1 V_{10}$.

For the pursuing collision, condition (20) gives an unrealistic result: $\delta < -1$.

Therefore, a more rapid particle always decelerates after a pursuing collision, by transferring a part of its momentum to the slower particle. In contrast, the same particle can accelerate, whatever its initial velocity, after a head-on collision, if condition (21) is satisfied. If this particle is of a very small mass ($\varepsilon \rightarrow 0$), then it can be accelerated even when the large particle is practically immobile ($\delta \ll 1$).

This mechanism forms the basis of the Fermi acceleration effect which is manifested within a large statistical ensemble of particles.

4.2. MECHANISM OF FERMI ACCELERATION IN A STATISTICAL ENSEMBLE

Let small particles (radionuclides) of the mass m_1 and velocity V_{10} cross a cloud of large particles (colloids) of a mass m_2 undergoing chaotic fluctuations at the characteristic velocity V_{02} . Let the condition (21) be satisfied, i.e., the large particles possess a mean fluctuation velocity that is not too low. The motion of a radionuclide within the cloud represents a chaotic walk caused by numerous collisions with colloids as schematically presented in Fig. 10.

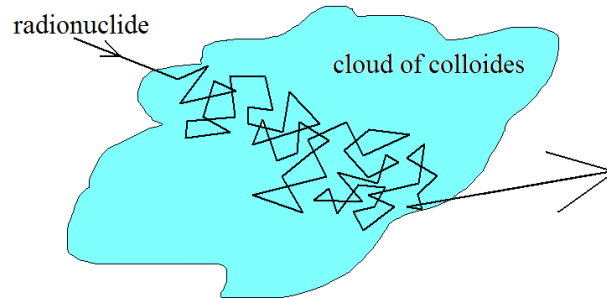


Figure 10. Acceleration of a small radionuclide particle after passing through the cloud of randomly walking colloid particles

In the big statistical ensemble of chaotically moving particles the probability of head-on collisions is higher than that of pursuing collisions. Indeed, let l be the characteristic distance between particles (the free-path length). Then the characteristic time between two head-on collisions is $\tau_h \sim l / (V_{10} + V_{20})$, whilst the characteristic time between two pursuing collisions is $\tau_{ov} \sim l / (V_{10} - V_{20})$. Obviously, $\tau_{ov} > \tau_h$. Therefore, during a fixed time interval the head-on collisions are more frequent than the pursuing ones. Taking into account that the pur-

suings collisions always decelerate small particles, while the head-on collisions accelerate them (provided that (21) is satisfied in each act), one concludes that the system of small particles randomly walking in the cloud of fluctuating large particles will be accelerated on average, until they leave the cloud. Thus, the characteristic velocity of small particles leaving the cloud is greater on average than their incoming velocity. This is the essence of the Fermi acceleration effect.

4.3. FERMI ACCELERATION AFTER MULTIPLE COLLISIONS

The described stochastic acceleration effect can be reached only if condition (21) is satisfied for each collision act. As mentioned above, this condition requires that the momentum of each large particle before collision would be greater than that of small particles. In practice this is observed only at the initial time instants just after the small particles penetrate in the cloud.

In the course of time each collision accelerating the small particles reduces the momentum of large particles, so that their momentum may become insufficient to overcome the threshold level needed to ensure acceleration in the consecutive collisions. In other words, for a set of consecutive collisions in time, one can expect a reduction of the stochastic acceleration and even its vanishing.

Due to this, the conditions needed to reach the acceleration after multiple consecutive collisions are expected to be stronger than (21).

These conditions may be obtained by examining the limiting behavior of a fluctuating particles in the cloud at large times when the dynamic equilibrium is set up. Such a limit state may then be analyzed in terms of statistical thermodynamics.

Let us assume that at large time after multiple collisions the cloud consists of two ensembles of fluctuating particles whose average absolute values of velocities are V_1 and V_2 . The initial average velocities at the moment when the small particles enter the cloud are V_{10} and V_{20} .

After multiple collisions the whole system will come eventually to the thermodynamic equilibrium when all particles have the same kinetic energy in average. So the following condition of the equilibrium:

$$m_1 V_1^2 = m_2 V_2^2 \quad (22)$$

The balance of kinetic energy for N_1 small particles and N_2 large particles is:

$$N_1 m_1 V_1^2 + N_2 m_2 V_2^2 = N_1 m_1 V_{10}^2 + N_2 m_2 V_{20}^2 \quad (23)$$

Then system (22) and (23) yields:

$$\omega^2 \equiv \frac{V_1^2}{V_{10}^2} = \frac{N_1 + \frac{N_2 m_2 V_{20}^2}{m_1 V_{10}^2}}{N_1 + N_2} \quad (24)$$

where ω is the velocity enhancement factor.

The necessary condition of acceleration is then:

$$\sqrt{\varepsilon} < \delta$$

where ε and δ are determined in section 4.2.

Thus, if two ensembles of particles of different masses, m_1 and m_2 , interact until the whole system comes to thermodynamic equilibrium, the condition of velocity increase in the subsystem of light particles is stronger than condition (21) for an unique collision.

4.4. ENHANCEMENT FACTOR FOR RADIONUCLIDE PARTICLES

To estimate the Fermi acceleration effect in real groundwater flow, it is reasonable to assume that the initial average velocities of both sorts of particles are approximately the same ($V_{01} \sim V_{02}$) and they are equal to the groundwater velocity. Then, as follows from Eq. (24), the equilibrium limit for the enhancement factor of the radionuclide velocity is:

$$\omega = \sqrt{\frac{\alpha\varepsilon + 1}{\alpha\varepsilon + \varepsilon}} \quad (25)$$

where $\alpha = N_1/N_2$.

The dependency of the enhancement factor on the relative concentration of particles α is shown in Fig. 11 for several values of the mass ratio ε .

As seen, the particle acceleration is reached when $\varepsilon < 1$. So, small particles are always accelerated under the examined conditions. All the curves located below the line $\omega = 1$ correspond to $\varepsilon > 1$.

To satisfy experimentally observed value $\omega \sim 1.5$, the following condition is deduced from (25):

$$\alpha \sim \frac{1}{5} \left(\frac{4}{\varepsilon} - 9 \right). \quad (26)$$

For small mass ratio, $\varepsilon \ll 1$, this formula gives $\alpha \approx \varepsilon^{-1}$.

It is seen that the Fermi acceleration mechanism can provide a significant velocity enhancement for small particles. In theory this effect can be much important than that observed in practice (see Fig. 11).

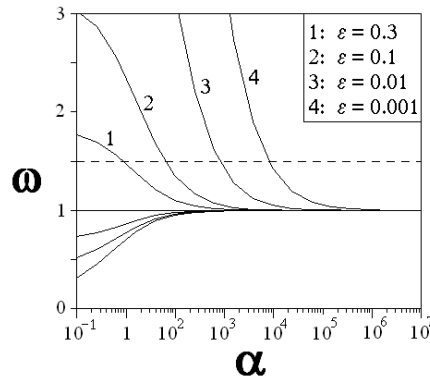


Figure 11. Radionuclide velocity enhancement factor versus relative concentration of particles $\alpha = N_1/N_2$ for several values of particle mass ratio ε

Sufficiently moderate values of ω observed experimentally may be explained by a so high concentrations of radionuclides that the energy of colloids is insufficient to accelerate all them. Another reason of the moderate acceleration is related to dissipation effects as well as inelastic collisions.

Discussion and Conclusion

The experimentally observed fact of a colloid/radionuclide transport velocity enhancement is usually explained by a size exclusion mechanism which implies that the radionuclides, being adsorbed on colloid particles, are only transported through the pores which are larger than a colloid particle, where the flow velocity is higher. In the present paper this ensemble of large pores accessible for colloids is called the *P - cluster*.

We suggest an improvement of this theory, by introducing three other effects which can either enhance the transport velocity or retard the transport. They are: friction-limited transport, percolation-breakup retardation, and the Fermi acceleration. All the effects were analyzed in terms of the velocity enhancement factor which is defined as the ratio between the particle average velocity and the total flow velocity.

The friction-limited transport predicts a transport retardation by the growth of the effective viscosity of the colloid suspension in large pores. The competition between the size exclusion effect and the friction-limited retardation reduces the effect of the velocity enhancement and even can lead to a resulting deceleration of the colloid transport if the colloid concentration and the particle size are sufficiently large.

Such a viscosity increase is significant for concentrated suspensions or sufficiently large particles. For diluted suspensions of fine particles this effect becomes of the same order as the volume exclusion or even less significant than the latter. Due to the competition between the size exclusion and the viscosity growth, the velocity enhancement is not observed for two cases (see Fig. 3): i) very fine particles ($\rho \ll 1$), for which all the particles can penetrate into all the pores; and ii) large overcritical particles ($\rho > \rho_{cr} > 1$) for which the effective viscosity growth becomes dominant. In this second case the particle transport is even retarded.

Using the model of a stochastic porous medium in the form of a capillary bundle of random radii, a qualitative model of the coupled radionuclide/colloid transport was developed, while taking into account the effective viscosity of the suspension. The velocity enhancement factor was defined in an analytical way and calculated for two various probability distributions for pore sizes. Both the effects of velocity enhancement and retardation can be observed, depending on the ratio between the colloid size and the mean pore diameter, as well as on the colloid concentration. A quantitative estimation obtained for the acceleration effect is in the agreement with the experimentally observed data.

It has been shown that various forms of the pore radii distributions produce qualitatively similar results for the velocity enhancement. The quantitative differences depend only on the length of the distribution "tail" that covers large pores: the longer the tail, the higher the velocity enhancement.

The effect of *percolation-breakup retardation* is related to the fact that the reduction of the ensemble of pores accessible to colloids due to a size-exclusion mechanism leads simultaneously to a reduction of the connectivity of this ensemble. Due to this the P -cluster can breakup its connectivity, which will totally stop the particle transport. This effect is modelled within the scope of the percolation theory, by using the 3D random capillary networks as the model of porous media. Using the numerical algorithms of selecting the random connected clusters, the enhancement factor was calculated numerically for several realizations of pore networks. It was shown that this effect reduces significantly the velocity enhancement factor, due to which its value cannot increase unlimitedly, as observed in practice. It is also shown that frequently this effect is not superposed with the friction-limited retardation, but suppresses it.

The effect of the *stochastic Fermi acceleration* predicts the probable acceleration on average of small radionuclides due to their elastic

collisions with colloid particles. This effect is observed only in the case when radionuclides are not absorbed on colloids. The mechanics of elastic collisions between particles of two different masses predicts two different results for two different kinds of collisions. The small particle (radionuclide) is always decelerated after a pursuing collision, and is preferably accelerated after a head-on collision due to a momentum transfer from the large particle (colloid). Such an acceleration happens only if the momentum of the colloid particle is sufficiently large.

In the statistical ensemble of fluctuating particles, the small particle will be accelerated on average as the pursuing collisions are less frequent than the head-on collisions. At the same time, due to each collision the large particles gradually lose their momentum, which reduces the acceleration effect in the course of time. A model of collisions is developed in the limit case of large time when the system reaches a kind of dynamic fluctuating equilibrium. The explicit relation is obtained for the limit enhancement factor of radionuclides which depends on the ratios of particle masses, velocities and concentrations. The initial condition imposed on the average particle momentum and ensuring the velocity enhancement is shown to be stronger for particle ensemble than for an individual collision act. The theoretical Fermi effect is capable to produce a much more important velocity enhancement than that observed in practice. Such a moderate enhancement can be explained by a sufficiently high radionuclide concentrations in groundflow, the inelastic nature of true collisions and other dissipative effects.

Acknowledgments

This research, initiated during the visit of Y.A. Stepanyants to the Institut National Polytechnique, Nancy, France (2003), was financed by the Groupement de Recherche MOMAS: Modélisation Mathématique et Simulations Numériques liées aux études d'entrepasage souterrain de déchets radioactifs (CNRS, ANDRA, EDF, CEA, BRGM) and by the Groundwater Project of ANSTO Environment (Australia).

References

- Bakhvalov, N.S., and Panasenko, G.P. *Homogenization : Averaging Processes in Periodic Media*. Kluwer Academic Publishers, Dordrecht, 1989.
- Buddemeier, R.W., and Hunt, J.R. Transport of colloidal contaminants in groundwater: Radionuclide migration at the Nevada test site. *Appl. Geochem.*, 3, 1988, 535–548.

- Benamar, A., Wang, H., Ahfir, N., Alem, A., Masséi, N. and Dupont, J.-P.: 2005, Effets de la vitesse d'écoulement sur le transport et la cinétique de dépôt de particules en suspension en milieu poreux saturé, *Géosciences de surface (Hydrologie – Hydrogéologie)*. *C.R. Geoscience* **337**, 497-504.
- Corapcioglu, M.Y. and Jiang, S.: 1993, Colloid-facilitated groundwater contaminant transport, *Water Resources Research* **29**(7), 2215-2226.
- Dodds, J.: 1982, La chromatographie hydrodynamique, *Analysis* **10**(3), 109-119.
- Entov, V., Feldman, Z., and Chen-Sin, E.: 1975. Simulation of the capillary imbibition in porous media. *Programmation*, 3, 67-74 (in Russian).
- Gilham, J. R., and MacMillan, D. J.: 1987, Improved interpretation of the inaccessible pore-volume phenomenon, *SPE Formation Evaluation*, 442-448.
- Grolimund D., Elimelech M., Borkovec M., Barmettler K., Kretzschmar R. and Sticher H.: 1998, Transport of in situ mobilized colloidal particles in packed soil columns, *Environmental Science & Technology* **32**, 3562-3569.
- Grolimund, D., Borkovec, M., Barmettler, K. and Sticher, H.: 1996, Colloid-facilitated transport of strongly sorbing contaminants in natural porous media: a laboratory column study, *Environmental Science & Technology* **30**, 3118-3123.
- Happel, J., and Brenner, H. *Low Reynolds hydrodynamics with special applications to particulate media*. Prentice-Hall, 1965.
- James, S.C., and Chrysikopoulos, C.V.: 2003, Effective velocity and effective dispersion coefficient for finite-sized particles flowing in a uniform fracture, *Journal of Colloid and Interface Science* **263**, 288-295.
- Kersting, A.B., Efurud, D.W., Finnegan, D.L., Rokop, D.J., Smith, D.K., and Thompson, J.L.: 1999, Migration of plutonium in groundwater at the Nevada Test Site, *Nature* **397**, 56-59.
- Kim, Zeh, P., and Delakovitz, B. Chemical interactions of actinide ions with groundwater colloids in Gorleben aquifer systems. *Radiochim. Acta*, 58-59, 1992, 147-154.
- Landau, L.D. and Lifshitz, E.M.: 1988, *Hydrodynamics*, Nauka, Moscow (in Russian). Engl. Transl.: *Fluid Mechanics*, Pergamon Press, Oxford, 1993.
- Landau, L.D., and Lifshitz, E. M. *Statistical Physics, Course of Theoretical Physics. Volume 5*, 3d ed., Pergamon Press, Oxford, 1980.
- Lieser, K.H., Ament, A., Hill, R., Singh, R.N., Singl, U., and Trybush, B. Colloids in groundwater and their influence on migration of trace elements and radionuclides. *Radiochim. Acta*, 49, 1990, 83-100.
- Logan, J. D.: 2001, *Transport modeling in hydrogeo-chemical systems. Interdisciplinary applied mathematics*, Springer-Verlag, New-York Inc.
- Mantoglou, A., and Wilson, J.L.: 1982, The turning bands method for simulation of random fields using line generation by a spectral method, *Water Resources Research* **18**(5), 1379-1394.
- Massei, N., Lacroix, M., Wang, H.Q., and Dupont, J.-P.: 2002, Transport of particulate material and dissolved tracer in a highly permeable porous medium: comparison of the transfer parameters, *Journal of Contaminant Hydrology* **57**, 21-39.
- McCarthy, J. F., and Zachara, J.M.: 1989, Subsurface transport of contaminants, *Environmental Science & Technology* **23**, 496-502.
- Moridis, G.J., Hu, Q., Wu, Y.-S., and Bodvarsson, G.S.: 2003, Preliminary 3-D site-scale studies of radioactive colloid transport in the unsaturated zone at Yucca Mountain, Nevada, *Journal of Contaminant Hydrology* **60**, 251-286.
- Oh, Wonho: 1998, *Random field simulation and an application of kriging to image thresholding*, Dissertation, State University of New York.

- Panfilova, I.: 2003, Ecoulements diphasiques en milieux poreux: modèle de ménisque, Thèse, Institut National Polytechnique de Lorraine, Nancy, 2003.
- Panfilova, I., and Panfilov, M.: 2000. New model of two-phase flow through porous media in a vector field of capillary forces. In: *Porous Media: Physics, Models, Simulation (Procs. Int. Conf)*, World Scientific Publishing, Singapore, 145-165
- Penrose, W.R., Polzer, W.L., Essington, E.N., Nelson, D.M., and Orlandini, K.A.: 1990, Mobility of plutonium and americium through a shallow aquifer in a semiarid region, *Environmental Science & Technology* **24**, 228-234.
- Pope, G. A.: 1980, The application of fractional flow theory to enhanced oil recovery. *Soc. Petrol. Eng. J.* **20**, 191-205.
- Ryan, J.N., and Elimelech, M.: 1996, Colloid mobilization and transport in groundwater. *Colloids Surfaces, A: Physicochemical and Engineering Aspects*, **107**, 1-56.
- Sagdeev, R. Z., Usikov, D. A., and Zaslavsky, G. M. *Nonlinear Physics. From the Pendulum to Turbulence and Chaos*. Harwood Academic Publishers, NY, 1988.
- Sen, T.K., and Khilar, K.C.: 2006, Review on subsurface colloids and colloid-associated contaminant transport in saturated porous media, *Advances in Colloid and Interface Science* **119**(2006), 71-96.
- Small, H.: 1974, Hydrodynamic chromatography, a technique for size analysis of colloidal particles. *J. Colloid Interface Sci.* **48**, 147-161.
- Sorbie, K. S.: 1991, *Polymer-Improved Oil Recovery*. Blackie, Glasgow.
- Sorbie, K. S., Parker, A. and Clifford, P. J.: 1987, Experimental and theoretical study of polymer flow in porous media, *SPE Reservoir Eng.*, August, 281-304.
- Teeuw, D. and Hesseling, F. Th.: 1980, Power-law flow and hydrodynamic behaviour of polymer solutions in porous media, *Paper SPE-8982*, 73-82.
- Van de Weerd, H., and Leijnse, A. Assesment of the effect of kinetics on colloid facilitated radionuclide transport in porous media. *J. Contam. Hydrol.*, **26**, 1997, 245-256.
- Von Gunten, H.R., Waber, U.E., and Krabenbuhl, U.: 1988, The reactor accident at Chernobyl: A possibility to test colloid-controlled transport of radionuclide in a shallow aquifer. *J. Contam. Hydrol.*, **2**, 237-247.
- Zaslavsky, G. M. *Chaos in Dynamic Systems*. Harwood Academic Publishers, NY, 1985.

